AIAA JOURNAL
Vol. 48, No. 10, October 2010

Factorial Design Experiment to Analyze the Response of a Luminescent Photoelastic Coating

Daniel R. Gerber* and James P. Hubner†
University of Alabama in Tuscaloosa, Tuscaloosa, Alabama 35487

DOI: 10.2514/1.J050060

A luminescent photoelastic coating is a relatively new technique to measure full-field surface strain and determine principal strain directions that has many potential applications in engineering. Generally, luminescent photoelastic coating technology uses an in situ strain gage measurement to calibrate the detected optical response to maximum shear strain. This calibration requires the determination of two coating parameters: the polarization efficiency and the coating characteristic. A better understanding and modeling of these two parameters, particularly the polarization efficiency, will enable a simpler a priori calibration and greater measurement accuracy. This paper presents a factorial design experiment that assesses the effect of four factors on the optical strain response of an luminescent photoelastic coating. The factors examined were substrate reflectance, luminescent dye concentration, absorption dye concentration and cure time. Results show the polarization efficiency is strongly correlated with the emission anisotropy of the coating. When the polarization efficiency is modeled as the measured emission anisotropy, the two most significant factors are the substrate reflectance and the luminescent dye concentration. Absorption dye concentration and reflectance-luminescence interaction are minor but significant effects. The most significant tested factors in modeling the coating coefficient are absorption dye concentration and substrate reflectance. The resulting uncertainties for the polarization efficiency and coating characteristic are 1.3 and 3.7%, respectively.

Nomenclature

a	=	absorptivity
E	=	modulus of elasticity
F	=	magnitude of the optical strain response
G	=	phase of the optical strain response
I	=	measured intensity
I_{avg}	=	average intensity over 180° analyzer rotation
$I_{\|\|}$	=	measured intensity using a vertical polarizer and a vertical analyzer
$I_{\perp}$	=	measured intensity using a vertical polarizer and a horizontal analyzer
K	=	optical sensitivity coefficient
N	=	sample size
n	=	degrees of freedom
r	=	emission (or fluorescence) anisotropy
U	=	uncertainty
α	=	analyzer angle
γ	=	maximum planar shear strain
η	=	coating characteristic
λ	=	excitation or emission wavelength
λ^*	=	effective wavelength, $\lambda_{em}\lambda_{ex}/(\lambda_{em} + \lambda_{ex})$
ν	=	Poisson ratio
σ	=	standard deviation
Φ	=	polarization efficiency

I. Introduction

AN ESSENTIAL step in the design process of all products containing structural components is stress analysis. Effective stress analysis of the components will ensure material- and cost-efficient designs and consistently safe operation. Common stress analysis methods range from experimental, pointwise techniques such as strain gages used in conjunction with constitutive equations to computational, three-dimensional techniques such as finite element analysis (FEA). A number of full-field experimental measurement techniques offer high spatial resolution but lower strain resolution, including photoelastic coatings, Moiré and interferometric methods, speckle methods and digital image correlation [1,2]. Each of these has advantages and disadvantages which make them suitable for differing applications; Olden and Patterson [3] present a rational decision making model to assist in the selection process.

Photoelasticity and corresponding coating techniques are common strain measurement techniques used by the aerospace industry for design and numerical analysis validation [4–6]. The luminescent photoelastic coating (LPC) technique is a strain measurement method for acquiring full-field, in-plane maximum shear strain and principal strain directions on the surface of the structural component [7,8]. The luminescence from the coating creates a more uniform emission field at oblique incidence compared with the reflected field of traditional reflective photoelastic coatings, enabling the potential of principal strain separation over the imaged field using oblique excitation [9].

An LPC consists of a luminescent dye and an absorption dye in a photoelastic binder. When a strained specimen coated with an LPC is illuminated by circular polarized light, as shown in Fig. 1, the strain-induced change of the polarization is partially retained by the luminescent emission [7]. As with all birefringent coatings [10], the change of the polarization is related to the maximum shear strain on the specimen. This relationship for an LPC is the optical strain response (OSR) and is defined in Sec. II. To measure the OSR, a charge-coupled device (CCD) camera with an analyzer placed in front of the lens acquires images of the emission at multiple analyzer angles. This sequence of images is captured once for the unloaded state and again for the load-applied state. These images are processed by a software program that determines the OSR. Calibration is then required to determine the relationship between the OSR and the maximum shear strain.

The current LPC technique typically relies on an in situ strain gage measurement to calibrate the OSR to the maximum shear strain. Either a uniaxial gage aligned along a known principal axis or a rosette gage is used to determine the calibrating maximum shear strain. The former requires knowledge of the material's properties. Various approaches of calibration are possible including gage

Presented as Paper 2010-0188 at the 48th AIAA Aerospace and Sciences Meeting, Orlando, FL, 4–7 January 2010; received 14 July 2009; revision received 7 July 2010; accepted for publication 7 July 2010.

*Undergraduate Research Assistant, Department of Mechanical Engineering, 290 Hardaway Hall. Student Member AIAA.

†Assistant Professor, Department of Aerospace Engineering and Mechanics, 215 Hardaway Hall. Associate Fellow AIAA.

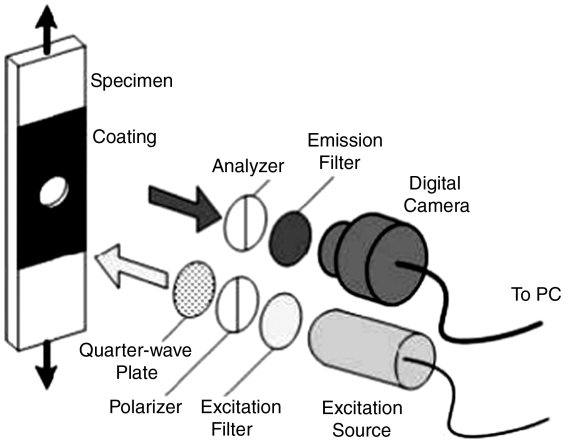

Fig. 1 Diagram of the LPC instrumentation.

measurements acquired on 1) an identical uncoated specimen if available or 2) the coated specimen after measuring the OSR and then removing an area of the coating, applying the gage and reloading the specimen. For simplified geometries with known analytical solutions, e.g., a cantilever beam, as is the case in this investigation, or a disk in compression, the OSR can be calibrated to the calculated maximum shear strain.

The relationship between the OSR and the maximum shear strain is determined by two coating parameters: the polarization efficiency and the coating characteristic. These are defined in Sec. II. A better understanding of these two coating parameters, particularly the polarization efficiency, is the focus of this investigation and will lead to greater measurement accuracy and potentially simpler a priori calibrations. This paper presents a factorial design experiment that assesses the effect of four factors on the calibration coefficients of an LPC. The four factors examined were substrate reflectance, luminescent dye concentration, absorption dye concentration and cure time. These factors were set to either a high or a low level in keeping with a factorial design of experiment. Further details as to why these factors were selected are discussed in Sec. III.

II. Theory

The emission of an LPC is characterized by [7]:

$$\frac{I}{I_{\text{avg}}} = 1 + F\sin(2\alpha - 2G) \tag{1}$$

where I is the total measured emission intensity, I_{avg} is the average measured emission intensity over 180° analyzer rotation, α is the analyzer angle, F is the magnitude of the OSR and G is the phase of the OSR. The OSR F is a function of the in-plane maximum shear strain γ and, for a single-layer luminescent photoelastic coating:

$$F = \Phi\frac{\gamma/\eta}{1 + (\gamma/\eta)^2} \tag{2}$$

where

$$\eta = \frac{a\lambda^*}{2\pi K} \tag{3}$$

The OSR of the coating adhered to the loaded specimen is measured by the imaging system in Fig. 1. To determine the corresponding maximum shear strain, the polarization efficiency Φ and coating characteristic η must be determined in situ by calibration or known a priori. While the latter is easier to implement if known, the former is more accurate, assisting in the elimination of systematic errors that can arise from batch variance, surface reflectance, and environment dependencies.

The coating characteristic is a function of the absorptivity a, the effective wavelength λ^*, as defined in the Nomenclature, and the optical sensitivity coefficient K. The absorptivity is a property of the absorption dye; higher absorptivity decreases the penetration depth of the excitation and reduces the coating thickness required for thickness-independent measurements [8]. The effective wavelength depends on the excitation and emission wavelengths of the luminescent dye and, thus, the excitation and emission filters used by the optical measurement system. The optical sensitivity coefficient of a photoelastic coating is a measure of the birefringent response of the binder to strain [10]. For an in situ calibration, these values are not measured independently but collectively as the coating characteristic. This is similar to the gage factor of an electrical-resistant strain gage being a function of alloy Poisson ratio and alloy resistivity. The coating characteristic can be thought of as a characteristic strain value that affects the curvature and sensitivity of the OSR. The value of η corresponds to the maximum shear strain of the peak OSR. A larger coating characteristic decreases the OSR sensitivity but extends its range, as shown in Fig. 2.

The polarization efficiency of the coating is related to the polarization retention of the luminescence. If the luminescence does not retain the strain-induced polarization changes of the excitation passing through the coating, then the emitting intensity will be depolarized and the measured intensity with respect to the analyzer position will be constant. For this case, the polarization efficiency is theoretically zero. Changes in the value of the polarization efficiency affect the maximum value the OSR curve reaches (also shown in Fig. 2). The polarization retention of luminescence depends on processes such as photoselection and depolarization [11]. A desired result is to determine how the polarization efficiency is related to measures of polarization retention.

Such a measure of polarization retention is the emission anisotropy [11] r, which is related to the orientation of the luminophors and $I_\perp$ and $I_{||}$:

$$r = \frac{1 - I_\perp/I_{||}}{1 + 2(I_\perp/I_{||})} \tag{4}$$

where $I_\perp$ represents the average intensity of an image taken with the emission analyzer orientation perpendicular to a linear excitation polarizer orientation and $I_{||}$ represents the average intensity of an image where the two orientations are parallel. Emission anisotropy (or simply anisotropy) originates due to the selective absorption and emission of a luminophor relative to the polarization state of the excitation and the transition moment of the luminophor. While a single luminophor can achieve an anisotropy of 1, the maximum anisotropy for randomly distributed luminophors without depolarization effects is 0.4 due to photoselection: the process of exciting luminophors that are partially aligned with the polarization of the excitation. Depolarization effects such as light scattering and reabsorption can further increase or decrease the response, respectively. Because the polarization efficiency depends on the polarization retention of the luminescent dye and anisotropy is an intensity-independent measure of polarization, these are expected to be related.

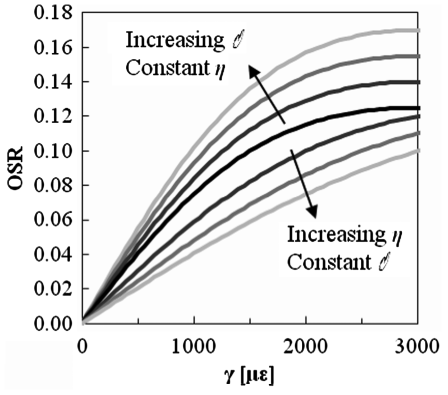

Fig. 2 Graph of OSR and shear strain for various values of Φ and η.

III. Experimental Technique

To measure the OSR, coated aluminum beam specimens were placed in a cantilever bending rig with a bending length of 254 mm, as shown in Fig. 3. Beam properties were $E = 70$ GPa, $\nu = 0.33$, thickness $= 6.26$ mm and width $= 25.4$ mm. This experiment was designed in a 2^k factorial method [12] with $k = 4$. In this design, a specimen was coated with each of the possible factor combinations for 16 total specimens. Four factors were varied: factor A, substrate reflectance, factor B, luminescent dye concentration, factor C, absorption dye concentration, and factor D, cure time.

The values for the factors were aggressively spaced at either 50% below (factors B and D) or 100% above (factor C) baseline values to ensure that the single-replicate factorial design of this experiment would provide accurate estimates of the effects of each. Aggressive spacing assists in distinguishing reliable effect estimates from noise. Center-point replicates, which would have modeled quadratic effects and provided a better response curve calibration, i.e., modeling of main and interaction effects, were not acquired because the mere detection of the presence of a relationship between the factors and the response was the objective of this investigation, not the response curve itself.

The substrate reflectance refers to whether or not the specimen was anodized black. This factor was selected because prior experience with the measurement technique by the investigators had shown that the surface background can affect the measured OSR. This arises from the reflectance of the emission and not the excitation because the image bandpass filter blocks the excitation. The reflectance of emission will likely affect the polarization efficiency due to the increase in the imaged intensity and decrease polarization retention when the substrate is more reflective. Two reflective conditions were selected: anodized black (1) and natural metallic (−1). For both cases, the specimen was lightly sandblasted with fine grit before the coating application to create a diffuse surface, remove surface contaminants and ensure a uniform surface texture.

The luminescent dye was decreased 50% by weight (−1) relative to the normal concentration (1). By lowering the concentration, the intensity of the luminescence will decrease, necessitating longer exposure times but possibly increasing the polarization retention due to a decrease of excitation crosstalk between luminophors [11]. The absorption dye was increased 100% by weight (1) relative to the normal concentration (−1). As apparent in Eq. (3), increasing the absorption dye concentration, hence, coating absorptivity, should increase the coating characteristic. This in turn will decrease the measurement sensitivity but increase the measurement range. Additionally, the greater the excitation absorption, the thinner the coating can be applied to the surface of the specimen and maintain thickness independent response [8]. Without the absorption dye, the relative retardation (or strain response) is thickness dependent and measurements of OSR would need to be corrected for coating thickness. A tradeoff of higher absorptivity is less detected luminescence, hence longer exposure times, due to less penetrating excitation. The expected affect of absorptivity on polarization efficiency is unknown.

The two cure times were a low cure time of 6 h (−1) and a high cure time of 12 h (1). The 12 h (overnight) cure is the normal protocol, and the interest in this factor is simply to determine if the cure time can be reduced without affecting the response of the coating.

A specimen was created for each combination of these four factors. First, the specimens were lightly sandblasted. Then, half of the specimens were anodized black. The specific coating solution was then prepared and applied to each specimen using an airbrush with a predetermined volume of the solution to assist in an even and consistent coating thickness among the specimens. Figure 4 shows a cube diagram of this experimental design. During the coating application process, the specimens were periodically flash-cured under ultraviolet (UV) light for a cumulative total of ∼20 min. This assists in deterring uneven buildup or runs during successive applications, particularly for three-dimensional objects. Once the coating had been completely applied, the specimens were placed under UV light for a final cure, either 6 or 12 h. The curing process occurred in the open laboratory at 20–22°C and 60–70% relative humidity.

Once the coating had been cured, each specimen was inspected to assure complete even and smooth surfaces free of ridges, excessive waviness and surface delimination. If a coating did not pass the visual inspection for coating quality, the coating was removed, the specimen was cleaned and a new coating was applied. The coating thickness was measured by averaging readings from a contact eddy-current probe at 12 points across the coated area (four points along vertical lines at 25, 50, and 75% of the width). The average coating thickness was 440 μm. The average thickness-coefficient-of-variance for a specific specimen was 7%. The coefficient-of-variance of the average-thickness for the full sample set was 10%. The presence of the absorption dye creates a negligible thickness-dependent measurement as long as a threshold thickness is achieved [8]: ∼350 μm for the base coating used in this investigation. Coatings that are too thin or exhibit excessive waviness or poor bond strength (noticeable delimination) will severely reduce measurement accuracy.

The specimens were tested in a randomized order to protect against systematic errors. The experimental design was orthogonal, but blocking was not performed. The tests were conducted by a single operator over multiple days. Multiday testing could result in environmental nuisance factors contributing to the measurements. However, the tests were conducted in a relatively controlled environment similar to the conditions of the curing environment. For temperatures less than 35°C, the optical sensitivity and emission anisotropy, which are related to the coating characteristic and polarization efficiency, respectively, are relatively stable [13]; thus, small changes in the environmental conditions were not expected to play a significant role.

The specimens were excited by circularly polarized light from a blue LED lamp (465 nm center wavelength) and images were acquired for both the unloaded and load-applied states. A scientific-grade (16-bit dynamic range, 100 ke$^-$) 1024 × 1024 CCD camera captured the images with a 600 nm filter (40 nm bandpass) attached to the 50 mm imaging lens. The LED lamp and camera were positioned next to each other and 1 m from the specimen. Power for the LED lamp, exposure time of the camera and the analyzer angle were all controlled with a LabVIEW software suite written specifically for

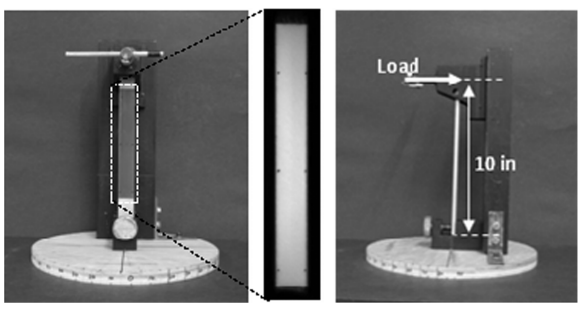

Fig. 3 Front and side photographs of specimen in testing rig and unprocessed intensity image (center) of the LPC luminescent emission (dashed area).

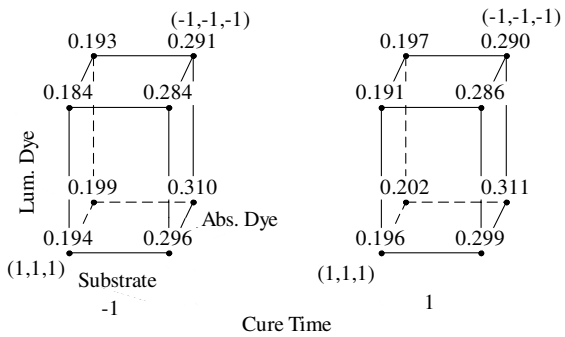

Fig. 4 Cube diagram of the experimental design and corresponding emission anisotropy values.

use with the LPC technique. Images were acquired (example image shown in Fig. 3) at eight analyzer angles separated by an interval of 22.5°. This sequence of images was acquired for both the unloaded state and the load-applied state. A dark-field image was also acquired with each test to correct for the values of the residual voltage in the camera pixels. The intensities of the image sequences were then fitted to a sinusoidal curve, shown in Fig. 5, to determine the OSR and phase, as per Eq. (1). The OSR test was performed twice for each specimen.

After completing the OSR measurements, the anisotropy was measured. With the specimen in the unloaded state and a linear polarizer attached to the LED lamp, one image was acquired with the analyzer oriented parallel to the direction of the polarizer and another was acquired with the analyzer perpendicular to the direction of the polarizer. These images were processed by the same software to determine the anisotropy [Eq. (4)].

IV. Results and Discussion

A nonlinear regression that employed the Levenberg–Marquardt (LM) algorithm was performed to calculate the best-fit values of the polarization efficiency and the coating characteristic in Eq. (2) by minimizing the mean square error between the fitted and measured OSR. The LM algorithm required an input range for both parameters to ensure realistic values. The maximum shear strain was determined based on linear beam theory, specimen properties and geometry and the applied beam deflection. As an example of the fit, Fig. 6 shows both the measured and best-fit OSR for specimen 12. Because of test duplication, averaged polarization efficiency and coating characteristic values were calculated and used in the analysis. Table 1 lists the best-fit polarization efficiency and coating characteristic calibration constants for each specimen and corresponding coded factors. Also listed is the emission anisotropy. The far-right column will be discussed later in this section.

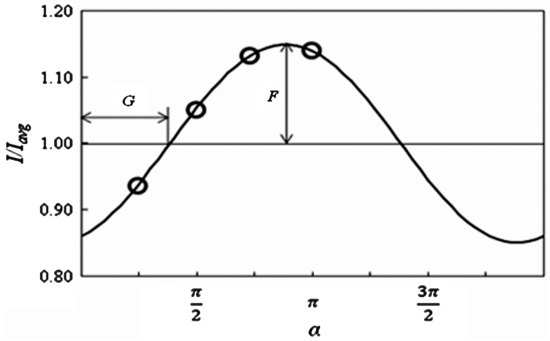

Fig. 5 Graph of Eq. (1) with the OSR *F* and the phase *G*, labeled. Circles represent a sequence of four images.

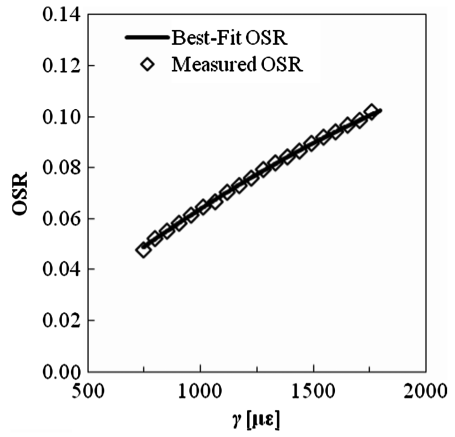

Fig. 6 Graph of the measured OSR (symbol) and best-fit curve based on Eq. (2).

Table 1 Polarization efficiency and coating characteristic best-fit values

Specimen	A^a	B	C	D	Φ	η	r	$\eta\,(\Phi = r)$
1	−1	−1	−1	−1	0.207	4095	0.194	3766
2	1	−1	−1	−1	0.260	3556	0.296	4181
3	−1	1	−1	−1	0.198	4132	0.184	3759
4	1	1	−1	−1	0.306	4633	0.284	4210
5	−1	−1	1	−1	0.233	6233	0.199	5198
6	1	−1	1	−1	0.297	5838	0.310	5690
7	−1	1	1	−1	0.164	4143	0.193	5035
8	1	1	1	−1	0.255	5288	0.291	6122
9	−1	−1	−1	1	0.185	3608	0.196	3885
10	1	−1	−1	1	0.270	3783	0.299	4296
11	−1	1	−1	1	0.157	2984	0.191	3884
12	1	1	−1	1	0.285	4343	0.286	4348
13	−1	−1	1	1	0.210	5508	0.202	5263
14	1	−1	1	1	0.309	5489	0.311	5512
15	−1	1	1	1	0.159	3976	0.197	5151
16	1	1	1	1	0.279	5251	0.290	5510

[a]A represents substrate reflectance, B is luminescent dye concentration, C is absorptive dye concentration, and D is cure time.

Statistical analysis was performed using the software suite Minitab and the best-fit Φ and η values calculated with the LM regression algorithm. The software created half-normal percentage probability plots for Φ and η (Figs. 7a and 7b, respectively) that provide an indication of which factors have a significant effect on the response variable. The criterion for statistical significance, or α level, was 5% for both graphs. A linear placement of the effects on the half-normal probability plot indicates a normal distribution of the effects and, thus, no significance. Any points that lie far from the linear distribution (in this case, the best-fit line) are not part of the normal distribution and, therefore, significant.

Based on the best-fit values of Φ and η using Eq. (2), substrate reflectance is the only significant factor for polarization efficiency and absorption dye concentration is the only significant factor for the coating characteristic; i.e. the probability of recording these effects based on a random effect for those factors is less than 5%. This can be seen in Figs. 7a and 7b by the distance points *A* and *C* lie from the normal probability line. It is important to note that although other points do not fall on the line, the large variance in effects prevents them from registering as statistically significant.

Given the sample size ($N = 16$) and effect of each factor, a t value can be calculated that describes the placement of that effect in a normal distribution of effects for a sample. A p value, or probability value, can then be determined. The p value is the probability that if the true effect of a given factor was insignificant, or normally distributed, then the recorded effect would have been observed. Thus, small p values indicate statistical significance. For the polarization efficiency, the t value for substrate reflectance is 7.70. This corresponds to a p value of less than 0.001, indicating that the substrate reflectance does indeed have a large effect on the polarization efficiency. Absolute values above $t_{0.05,14} = 2.14$ indicate significance where 14 represents the degrees of freedom n, due

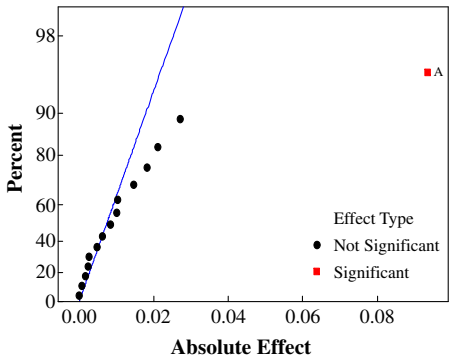

Fig. 7 Graphs of half-normal % probability plot for a) the polarization efficiency Φ; and b) the coating characteristic η.

to the inclusion of one significant effect and the sample average. For the coating characteristic, the t value and p value for the effect of absorption dye concentration are 3.99 and 0.001, respectively, indicating that the factor does have a significant effect on the parameter.

A regression model for each parameter using the detected significant factors, one each for Φ and η, was generated. Because this is a 2^k factorial design without center-point replicates, the regression model does not have quadratic or higher-order terms such as A^2 or B^2, but can contain interaction terms such as AB if significant. A comparison of observed versus expected values (Figs. 8a and 8b for Φ and η, respectively) shows that neither of the regression models developed is accurate, not unexpected because only one effect was retained for each parameter. This inaccuracy stems directly from the large variance in effects seen in Figs. 7a and 7b. Figure 9 displays a likely cause of this variance. The mean square error (MSE) topology of the OSR shows a large region of ordered pairs (Φ, η) that correspond to a low MSE (the dark trough extending from lower left to upper right of Fig. 9). In this instance, the ordered pair (0.25, 5000) is the true state; however, the ordered pair (0.27, 5500) will also have a low MSE. Because of the shallow MSE gradient and the presence of measurement noise, it is possible to calculate values for both parameters using a two-parameter, nonlinear regression that minimizes the MSE but fails to accurately calculate each parameter individually.

An inspection of Table 1 reveals that the polarization efficiency and the anisotropy are approximately equal. The anisotropy is lower for unanodized specimens ($A = -1$) compared with the anodized specimens ($A = 1$). The polarization efficiency, Eq. (2), is a fitted calibration parameter of polarization retention. The anisotropy of Eq. (4) is a defined function of $I_{\perp}$ and $I_{||}$. When the polarization efficiency for each specimen is set equal to the measured anisotropy and only the values for the coating characteristic are recalculated using the LM algorithm, a clearer distinction between significant and not significant factors is found. The results for the coating characteristic when $\Phi = r$ are listed in the far-right column of Table 1.

The half-normal probability plots created for the new data (Figs. 10a and 10b) indicate more significant factors. Table 2 presents statistical results of the analysis including the effect size, t value, and p value for each significant factor or interaction. For the polarization efficiency, where four factors are significant, the t value for significance is 2.20. For the coating characteristic, the t value is 2.16. Also listed in Table 2 is the precision uncertainty in the Φ and η measures. The uncertainty for the two-level design was assessed using Eq. (5) [12]:

$$U = \pm \frac{4\sigma}{\sqrt{N}} \tag{5}$$

where σ represents the parameter standard deviation. Because multiple replicates were not acquired (there is only one sample specimen for each combination of factors), the value of the standard

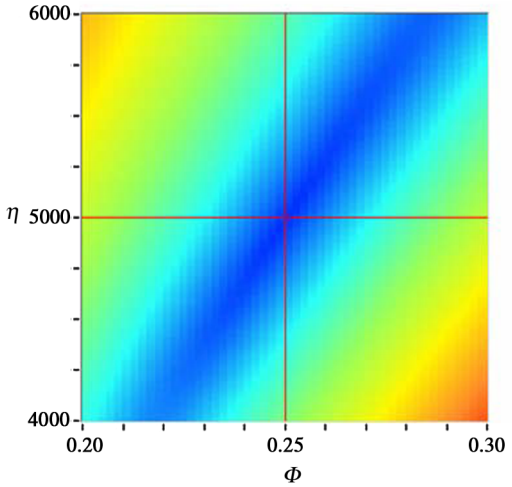

Fig. 9 Mean square error topology of a fitted data set for $\Phi = 0.25$ and $\eta = 5000$. Darker shading represents lower MSE.

deviation was estimated based on the effect size corresponding to the t value of significance. In terms of percentage relative to the average polarization efficiency and coating characteristic of the sample, the precision uncertainties are 1.3 and 3.6%, respectively. When calculating the polarization efficiency based on the emission anisotropy, two primary sources of bias uncertainty are camera shot noise and polarizer alignment. For the measurement system used in this experiment, these were 0.28 and 0.14%, respectively, for the intensity ratio $I_{\perp}/I_{||}$. Propagating the uncertainty based on Eq. (4), the bias uncertainty for the polarization efficiency is 0.16% when $\Phi = 0.25$. Compared with the precision uncertainty, this is negligible. The calculated bias uncertainty for the coating characteristic, dominated by strain uncertainty and calculated based on the geometry and deflection of the specimen, was 0.79%. Combined with the precision uncertainty, the total uncertainty in the coating characteristic is 3.7%.

For the first analysis case where both calibration constants were free to fit the experimental OSR and the resulting scatter was much larger, the polarization efficiency and coating characteristic precision uncertainties are 11 and 16%, respectively. When determining the polarization efficiency via two-parameter curve fit, three primary sources of bias uncertainty in the OSR are camera shot noise, excitation polarization and temperature. For the system used in this experiment, these were 0.2, 0.1, and 0.5%, respectively, assuming 1°C temperature drift. The combined bias uncertainty in the OSR resulted in a 0.55% uncertainty in polarization efficiency which is negligible compared with the 11% precision uncertainty.

Figures 11a and 11b show the residuals for the polarization efficiency and coating characteristic, respectively, for both analyses:

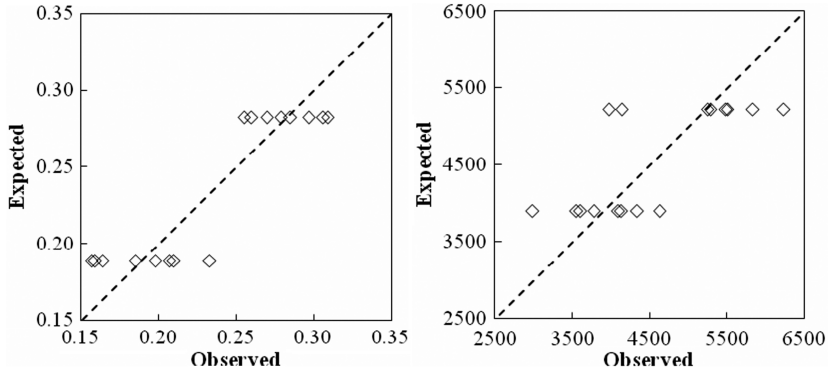

Fig. 8 Graphs of a) observed and expected values for the model created for the polarization efficiency considering substrate reflectance as the only significant factor; and b) observed and expected values for the model created for the coating characteristic considering absorption dye concentration as the only significant factor.

Table 2 Effect size and statistics of significant parameters when $\Phi = r$

Parameter	Factor	Effect	t value	p value	Uncertainty
Φ	A	0.1014	73.29	<0.001	0.0031
Φ	B	−0.0114	−8.22	<0.001	
Φ	C	0.0079	5.69	<0.001	
Φ	AB	−0.0049	−3.52	0.005	
η	A	491	6.24	<0.001	170
η	C	1394	17.71	<0.001	

Φ fit and $\Phi = r$. The residuals appear structureless, indicating a reasonable assumption of independence, except for a slight upward trend in the polarization efficiency residuals when $\Phi = r$. The residuals for the two-coefficient fit are larger on average as expected. When normalized by the standard error, the residuals for both analyses fall within two standard errors except for one point of the coating characteristic when $\Phi = r$. This point, which lies just outside of three standard errors, was retained in the analysis to maintain an orthogonal design but is likely one reason while the coating characteristic uncertainty is larger than the polarization uncertainty. The observed versus expected graphs (Figs. 12a and 12b) for the $\Phi = r$ analysis exhibit a much better correlation than Figs. 8a and 8b.

For the polarization efficiency, the substrate reflectance and luminescent dye concentration have major effects while the absorption dye concentration and the reflectance-luminescence interaction have minor effects. Higher polarization efficiency exists when the specimen is anodized. The higher polarization efficiency increases the sensitivity of the OSR to maximum shear strain. The lower polarization efficiency for the metallic specimens indicates that the reflection of the luminescence partially destroys the polarization. While the absolute image intensity increases for the metallic surface, the sensitivity is less. A flat black undercoat should provide the same effect as an anodized surface but compatibility and adhesion are other important factors to consider with an undercoat.

The luminescent dye is the second strongest effect on polarization efficiency, and the negative t value indicates an inverse correlation. Thus, in terms of sensitivity, lower concentration is preferred; however, decreased concentration will proportionally decrease the absolute measured intensity. This will increase relative imager shot-noise unless longer exposures times are used. The nature of this effect is possibly similar to the surface reflectance in that the stronger the luminescence (higher concentration) causes more surface reflection to be captured in the image. It could also be related to luminescence self-quenching at higher concentrations. The interaction effect of these two factors has a minor but significant negative correlation with polarization efficiency; the absorption dye concentration shows a minor positive correlation.

For the coating characteristic, the absorption dye concentration has a major effect and the substrate reflectance has a minor effect. The positive correlation with absorption dye concentration is expected; Eq. (3) is a function of absorptivity and adding more dye increases the excitation absorption. This effect decreases the OSR sensitivity but increases the range. The surface reflection affecting the coating characteristic is unexpected. While it cannot be determined from the design of this experiment how or if the reflected luminescence specifically affects the optical sensitivity or the effective wavelength of the coating, the other two variables of the coating characteristic in Eq. (3), the increase of the reflected luminescence of the metallic specimens causes a decrease in the coating characteristic.

All effects and interactions not listed in Table 2, including cure time and all its interactions, were deemed insignificant. The probability that these insignificant effects were judged as such

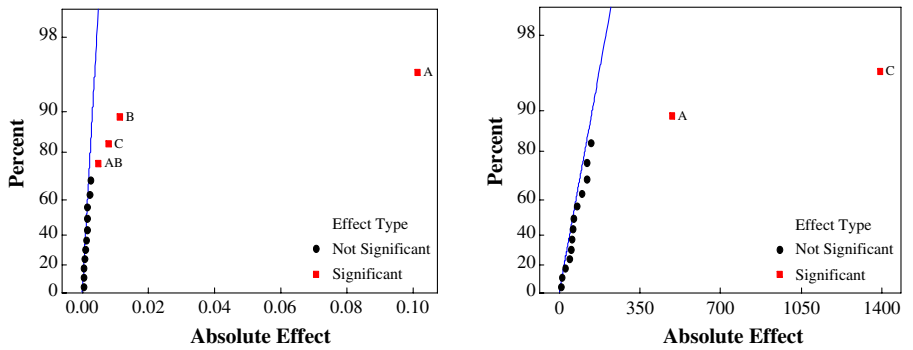

Fig. 10 Graphs of a) half-normal % probability plot for the polarization efficiency Φ when it is set equal to the anisotropy; and b) half-normal % probability plot for the coating characteristic η when polarization efficiency is set equal to the anisotropy.

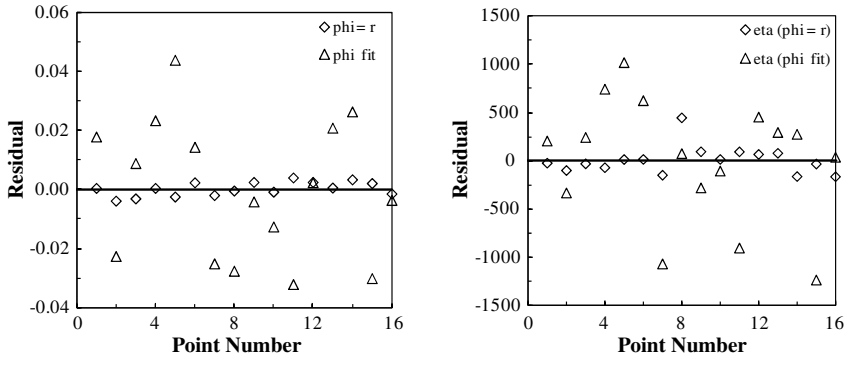

Fig. 11 Graphs of a) polarization efficiency residual plot for both analysis procedures; and b) coating characteristic residual plot for both analysis procedures.

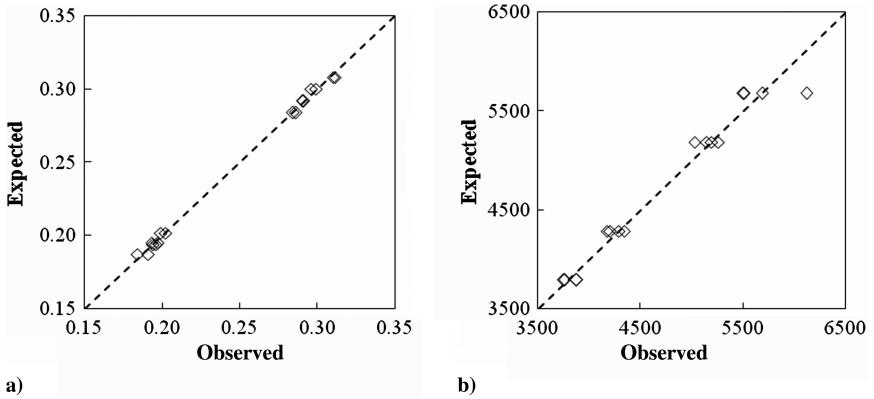

Fig. 12 Graphs of a) observed and expected values for the model created for the polarization efficiency set equal to the emission anisotropy; and b) observed and expected values for the model created for the coating characteristic when the polarization efficiency is set equal to the emission anisotropy.

erroneously, i.e., that they actually are significant despite being judged insignificant (type II or β error), was calculated with the highest order interaction ($ABCD$) neglected. For the polarization efficiency, the highest β error was 5.5% (D-cure time). For the coating characteristic, the highest β error was 3.0% for the CD interaction. If the cure effect and all its interactions are indeed insignificant, then the data can be analyzed as a 2^3 factorial with a hidden replicate. Analyzing the data as such results in the same significant effects in Table 2 but with slightly different t- and p-values. The largest β-errors increase to 37% for the ABC interaction of the polarization efficiency and 14% for AB interaction of the coating characteristic.

Because the independent measure of polarization efficiency leads to a better determination of the coating characteristic, current efforts are focused on understanding why the polarization efficiency should be equal to or closely approximated by the emission anisotropy. The model will include photoselection, the dependence of electric field absorption and emission based on luminophor orientation relative to the excitation, and depolarization as a weighted function of nonpolarized, diffuse emission.

V. Conclusions

A factorial design experiment was performed to assess the effects of variation in four coating factors on the optical strain response of a luminescent photoelastic coating. After testing 16 specimens with varied luminescent dye concentrations, absorption dye concentrations, substrate reflectance and cure times, and analyzing the results using statistical analysis software, only certain factors were found to have a significant effect on the polarization efficiency and the coating characteristic. Improved characterization of the calibration parameters was achieved when the polarization efficiency was set equal to the coating emission anisotropy and the coating characteristic was determined based on a nonlinear regression fit. The primary significant factors for the polarization efficiency and coating characteristic are substrate reflectance and absorption dye concentration, respectively. Lesser but significant factors affecting the polarization efficiency are luminescent dye concentration, absorption dye concentration and luminescence-reflectance interaction. The only minor factor for the coating characteristic is substrate reflectance. Cure time (6 or 12 hr) and all other interactions have no significant effect. The resulting uncertainties for the polarization efficiency and coating characteristic are 1.3 and 3.7%, respectively. These results will be used to guide the theoretical modeling of the polarization efficiency and coating characteristic of a luminescent photoelastic coating.

Acknowledgments

This research was supported by National Science Foundation contract CMMI-0643170, Shih-Chi Liu program manager, and the University of Alabama Computer-Based Honors Program. The authors also thank the assistance of Ergin Esirgemez in support of the project.

References

[1] Kobayashi, A. S. (ed.), *Handbook on Experimental Mechanics*, Prentice–Hall, Englewood Cliffs, NJ, 1987.

[2] Dally, J. W., and Riley, W. F., *Experimental Stress Analysis*, 4th ed., College House Enterprises, Knoxville, TN, 2004.

[3] Olden, E. J., and Patterson, E. A., "A Rational Decision Making Model for Experimental Mechanics," *Experimental Techniques*, Vol. 24, No. 4, 2000, pp. 26–32. doi:10.1111/j.1747-1567.2000.tb00922.x

[4] Slaminko, R., "Contributions of Photoelasticity to the Development of the Boeing 777," *Society for Experimental Mechanics Conference and Exhibition*, Society for Experimental Mechanics, Inc., Bethel, CT, June 1993.

[5] O'Brien, E. W., "Progress in experimental stress analysis for Airbus aircraft design," *Strain*, Vol. 31, No. 4, 1995, pp. 131–134. doi:10.1111/j.1475-1305.1995.tb00976.x

[6] Gambrell, S. C., "Photostress Analysis of the Lower Weld of an Aft Skirt of a Solid Rocket Booster," *Experimental Techniques*, Vol. 19, No. 4, 1995, pp. 13–16. doi:10.1111/j.1747-1567.1995.tb00864.x

[7] Hubner, J. P., Ifju, P. G., Schanze, K. S., Liu, Y., Chen, L., and El-Ratal, W., "Luminescent Photoelastic Coatings," *Experimental Mechanics*, Vol. 44, No. 4, 2004, pp. 416–424.

[8] Hubner, J., Chen, L., Liu, Y., Schanze, K., Nicolosi, J., Ifju, P., and El-Ratal, W., "Characterization of a New Luminescent Photoelastic Coating," *Experimental Mechanics*, Vol. 45, No. 2, 2005, pp. 137–143. doi:10.1007/BF02428186

[9] Takahashi, D., and Hubner, J. P., "Strain Separation on a Nonplanar Object Using a Luminescent Photoelastic Coating," *Experimental Mechanics*, Vol. 50, No. 3, 2010, pp. 365–375. doi:10.1007/s11340-009-9232-y

[10] Zandman, F. S., Redner, A. S., and Dally, J. W., *Photoelastic Coatings*, Iowa State Univ. Press, Ames, IA, 1977, pp. 31–35.

[11] Lakowicz, J. R., *Principles of Fluorescence Spectroscopy*, 3rd ed., Springer, New York, 2006, pp. 353–366.

[12] Montgomery, D. C., *Design and Analysis of Experiments*, 6th ed., Wiley, New York, 2005, pp. 203–253.

[13] Esirgemez, E., and Hubner, J. P., "Temperature Dependence of the Luminescent Photoelastic Coating Technique," *Journal of Strain Analysis for Engineering Design*, Vol. 44, No. 8, 2009, pp. 699–711. doi:10.1243/03093247JSA520

R. Kapania
Associate Editor